

# UC San Diego

## UC San Diego Previously Published Works

### Title

Structural Characterization of  $(C_5H_5)Co(PPh_3)(\eta^2\text{-alkyne})$  and  $(C_5H_5)Co(\eta^2\text{-alkyne})$  Complexes of Highly Polarized Alkynes

### Permalink

<https://escholarship.org/uc/item/1fq639zc>

### Journal

Organometallics, 32(19)

### ISSN

0276-7333

### Authors

Baldrige, Kim K  
Bunker, Kevin D  
Vélez, Carmen L  
et al.

### Publication Date

2013-10-14

### DOI

10.1021/om400749g

Peer reviewed

# Structural Characterization of $(C_5H_5)Co(PPh_3)(\eta^2\text{-alkyne})$ and $(C_5H_5)Co(\eta^2\text{-alkyne})$ Complexes of Highly Polarized Alkynes

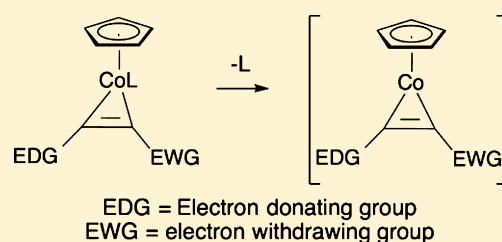
Kim K. Baldrige,<sup>\*,†</sup> Kevin D. Bunker,<sup>‡</sup> Carmen L. Vélez,<sup>‡</sup> Ryan L. Holland,<sup>‡</sup> Arnold L. Rheingold,<sup>‡</sup> Curtis E. Moore, and Joseph M. O'Connor<sup>\*,‡</sup>

<sup>†</sup>Institute of Organic Chemistry, University of Zürich, Winterthurerstrasse 190, CH-8057 Zürich, Switzerland

<sup>‡</sup>Department of Chemistry and Biochemistry (0358), University of California, San Diego, 9500 Gilman Drive, La Jolla, California 92093-0358, United States

## S Supporting Information

**ABSTRACT:** The solid state structures of the cobalt–alkyne complexes  $(\eta^5\text{-}C_5H_5)(PPh_3)Co\{\eta^2\text{-}(R_3Si)C\equiv C(SO_2Ar)\}$  (**3-TMS**, R = Me, Ar = C<sub>6</sub>H<sub>5</sub>; **3-TIPS**, R = CH(CH<sub>3</sub>)<sub>2</sub>, Ar = *p*-C<sub>6</sub>H<sub>4</sub>CH<sub>3</sub>) and the noncoordinated alkyne (Me<sub>3</sub>Si)C≡C(SO<sub>2</sub>Ph) (**6-TMS**) have been characterized by X-ray crystallography and, in the case of **3-TMS**, **6-TMS**, and  $(\eta^5\text{-}C_5H_5)Co\{\eta^2\text{-}(Me_3Si)C\equiv C(SO_2Ph)\}$  (**5-TMS-calc**), by B97D/Def2-TZVPP computational analysis. The phosphine-dissociated complex **5-TMS-calc** is determined to be a ground state singlet. Analysis of bond angle and distance metrics, calculated NMR chemical shift data, and molecular orbital analysis provide strong evidence for a four-electron-donor alkyne ligand in **5-TMS-calc**. The degree of asymmetry in metal–alkyne bonding, as defined by the Gladysz alkyne-slippage parameter, is dramatically reduced in **5-TMS-calc** relative to that in the precursor complex **3-TMS-calc**.



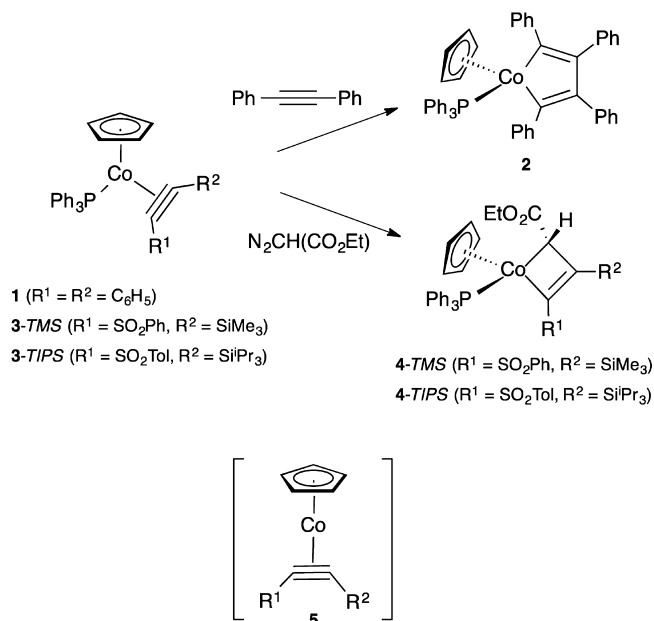
## INTRODUCTION

Metal–alkyne complexes continue to play a key role in the discovery and development of new organometallic reactions.<sup>1–3</sup> The first stable mononuclear cobalt–alkyne complex,  $(\eta^5\text{-}Cp)(PPh_3)Co(\eta^2\text{-}PhC\equiv CPh)$  (**1**; Cp = C<sub>5</sub>H<sub>5</sub>), was prepared over 45 years ago by Yamazaki and Hagihara, who also demonstrated the conversion of **1** and additional alkyne to a metallacyclopentadiene complex, **2** (Scheme 1).<sup>1a</sup> More recently it has been found that unsaturated four-membered-ring metallacycles are also accessible from  $(\eta^5\text{-}Cp)(PPh_3)Co(\eta^2\text{-alkyne})$  precursors via reaction with ethyl diazoacetate. For example, ethyl diazoacetate undergoes a diastereoselective oxidative cyclization with the unsymmetrically substituted alkyne complexes  $(\eta^5\text{-}Cp)(PPh_3)Co\{\eta^2\text{-}(R_3Si)C\equiv C(SO_2Ar)\}$  (**3-TMS**, Ar = C<sub>6</sub>H<sub>5</sub>, R = Me; **3-TIPS**, Ar = *p*-C<sub>6</sub>H<sub>4</sub>CH<sub>3</sub>, R = <sup>i</sup>Pr) to generate the metallacyclobutenes  $(\eta^5\text{-}Cp)(PPh_3)Co\{\kappa^2\text{-}CH(CO_2Et)(R_3Si)C=C(SO_2Ar)\}$  (**4-TMS**, Ar = C<sub>6</sub>H<sub>5</sub>, R = Me; **4-TIPS**, Ar = *p*-C<sub>6</sub>H<sub>4</sub>CH<sub>3</sub>, R = <sup>i</sup>Pr) with complete control of alkyne regiochemistry (Scheme 1).<sup>2</sup>

The reactions of  $(\eta^5\text{-}Cp)Co(PPh_3)(\eta^2\text{-alkyne})$  complexes, including the conversion of **3-TMS** to **4-TMS**, may involve the formation of phosphine-free  $(\eta^5\text{-}Cp)Co(\eta^2\text{-alkyne})$  (**5**) intermediates (Scheme 1); however, intermediates of this type have been neither observed nor isolated. It is therefore of interest to elucidate the structures of both the unsymmetrically substituted alkyne complexes, e.g. **3**, and the corresponding phosphine-dissociated analogues, **5**.

Here we report the first solid-state structures of  $(\eta^5\text{-}Cp)Co(PPh_3)(\eta^2\text{-alkyne})$  complexes bearing unsymmetrically substituted alkynes, **3-TMS** and **3-TIPS**, as well as computa-

## Scheme 1. Conversion of $(\eta^5\text{-}Cp)Co(PPh_3)(\eta^2\text{-alkyne})$ Complexes to Unsaturated Metallacycles



tional analysis of **3-TMS** and  $(\eta^5\text{-}C_5H_5)Co\{\eta^2\text{-}(TMS)C\equiv C(SO_2C_6H_5)\}$  (**5-TMS-calc**, TMS = SiMe<sub>3</sub>). The complex **5**-

Received: July 30, 2013

Published: September 13, 2013

*TMS-calc* exhibits a singlet ground state which compares to a previous report that  $(\eta^5\text{-C}_5\text{H}_5)\text{Co}(\eta^2\text{-HC}\equiv\text{CH})$  exists as a ground state triplet.<sup>3</sup> A comparison of the predicted structures for *3-TMS-calc* and *5-TMS-calc* supports the formulation of *5-TMS-calc* as electronically saturated due to involvement of a four-electron-donor alkyne ligand. The degree of alkyne-ligand slippage, as defined by the Gladysz slippage parameter,<sup>4</sup> is moderated significantly upon dissociation of the phosphine ligand from *3-TMS*.

## RESULTS AND DISCUSSION

**Structural Characterization of  $(\text{TMS})\text{C}\equiv\text{C}(\text{SO}_2\text{Ph})$  (*6-TMS*).** In order to determine the structural changes that occur

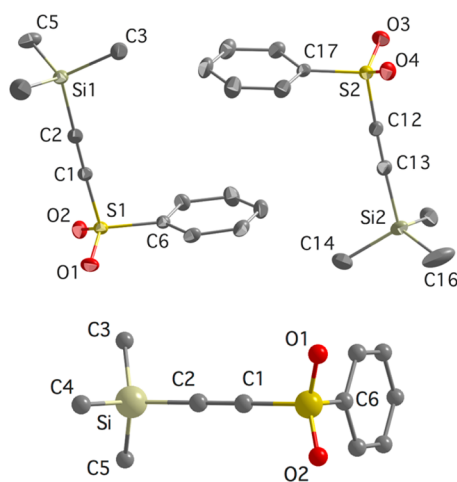


**Figure 1.** (top) ORTEP drawings of the two independent molecules in the crystal lattice of  $\text{Me}_3\text{SiC}\equiv\text{CSO}_2\text{Ph}$  (*6-TMS*). (bottom) Ball-and-stick drawing of the computed structure for *6-TMS-calc*. Hydrogen atoms are omitted for clarity.

**Table 1.** Selected Bond Distances (Å) and Angles (deg) for *6-TMS-calc* and *6-TMS* (Two Independent Molecules in the Unit Cell)

	<i>6-TMS-calc</i>	<i>6-TMS</i> (av)	<i>6-TMS-A</i> <sup>a</sup>	<i>6-TMS-B</i> <sup>a</sup>
C1(C12)–C2(C13)	1.2225	1.2014(19)	1.2033(18)	1.1995(19)
C1(C12)–S1(S2)	1.7270	1.7187(14)	1.7199(13)	1.7175(14)
C2(C13)–Si1(Si2)	1.8582	1.8686(14)	1.8698(14)	1.8674(14)
S1(S2)–C6(C17)	1.7915	1.7543(14)	1.7549(14)	1.7537(14)
S1(S2)–O1(O3)	1.4477	1.4332(11)	1.4314(11)	1.4351(11)
S1(S2)–O2(O4)	1.4477	1.4342(11)	1.4335(10)	1.4348(11)
C1(C12)–C2(C13)–Si1(Si2)	179.72	178.6(1)	179.1(1)	178.2(1)
C2(C13)–C1(C12)–Si1(Si2)	179.81	178.2(1)	178.3(1)	178.0(1)
C1(C12)–S1(S2)–C6(C17)	101.40	102.55(6)	101.85(6)	103.24(6)

<sup>a</sup>*6-TMS-A* is the S1/Si1 compound, and *6-TMS-B* is the S2/Si2 compound.

upon alkyne binding to cobalt, X-ray crystallographic and computational analysis of  $(\text{TMS})\text{C}\equiv\text{C}(\text{SO}_2\text{Ph})$  (*6-TMS* and *6-TMS-calc*) (Figure 1 and Table 1) was carried out. Good

**Table 2.** Selected Spectroscopic Data for Cobalt–Alkyne Complexes *1*, *3-TMS*, and *3-TIPS*

compd <sup>g</sup>	IR $\nu(\text{C}\equiv\text{C})$ <sup>a,b</sup>	<sup>1</sup> H NMR ( $\delta$ ) <sup>c</sup>	<sup>13</sup> C NMR ( $\delta$ ) <sup>c,d</sup>
[M] ( $\text{TMS}\text{C}\equiv\text{C}^1\text{SO}_2\text{Ph}$ ) ( <i>3-TMS</i> )	1772 <sup>e</sup> ( $\Delta = 338$ )	4.70 ( $\text{C}_5\text{H}_5$ ) 0.27 (TMS)	118.1 (C1), $J_{\text{PC}} = 11.6$ ( $\Delta = 17.2$ ) 105.5 (C2), $J_{\text{PC}} = 3.5$ ( $\Delta = 5.5$ )
[M]( $\text{TIPSC}\equiv\text{C}^1\text{SO}_2\text{Tol}$ ) ( <i>3-TIPS</i> )	1773 ( $\Delta = 348$ )	4.62 ( $\text{C}_5\text{H}_5$ ) 0.95 (TIPS) 1.12 (TIPS)	120.0 (C1), $J_{\text{PC}} = 13.7$ ( $\Delta = 17.1$ ) 100.5 (C2), $J_{\text{PC}} \approx 0$ ( $\Delta = 2.0$ )
[M]( $\text{PhC}\equiv\text{CPh}$ ) ( <b>1</b> ) <sup>10</sup>	1819 ( $\Delta = 403$ ) <sup>f</sup>	4.81 ( $\text{C}_5\text{H}_5$ )	90.4, $J_{\text{PC}} = 8.0$ ( $\Delta = 0.2$ )

<sup>a</sup>All IR data (in units of  $\text{cm}^{-1}$ ) were obtained from thin films on either KBr or NaCl plates, unless otherwise noted. <sup>b</sup>Values in parentheses are the differences in stretching frequencies between the free and coordinated alkynes. <sup>c</sup>NMR resonances were referenced to solvent peaks and observed at ambient temperature;  $J_{\text{PC}}$  values are given in Hz. <sup>d</sup>Values in parentheses are the chemical shift differences (ppm) of the sp carbons for the coordinated and noncoordinated alkynes. <sup>e</sup>In Nujol. <sup>f</sup>Free alkyne stretch from Raman spectrum. <sup>g</sup>[M] =  $\text{CpCo}(\text{PPh}_3)$ .

agreement is found between the experimental and B97D/Def2-TZVPP predicted structures for *6-TMS*, with an average C1–C2 triple-bond distance of 1.2014(19) Å in the solid-state structures and a 1.2105 Å distance in the predicted structure (Figure 1). The highly polarized nature of *6-TMS* ( $\sigma_p = 0.68$ ,  $\sigma_m = 0.62$  for  $\text{SO}_2\text{Ph}$ ;  $\sigma_p = -0.07$ ,  $\sigma_m = -0.04$  for TMS)<sup>5</sup> is confirmed by the calculated 5.7 D dipole moment. For comparison, the computed dipole moment of  $(\text{TMS})\text{C}\equiv\text{C}(\text{COMe})$  is 3.6 D.

**Synthesis and Spectroscopic Characterization of  $(\eta^5\text{-C}_5\text{H}_5)(\text{PPh}_3)\text{Co}\{\eta^2\text{-(R}_3\text{Si)C}\equiv\text{C}(\text{SO}_2\text{Ar})\}$  (*3-TMS*, R = Me, Ar =  $\text{C}_6\text{H}_5$ ; *3-TIPS*, R =  $\text{CH}(\text{CH}_3)_2$ , Ar =  $p\text{-C}_6\text{H}_4\text{CH}_3$ ).** As described previously,<sup>2</sup> the alkyne complexes *3-TMS* and *3-TIPS* were prepared from  $(\eta^5\text{-C}_5\text{H}_5)\text{Co}(\text{PPh}_3)_2$  and the corresponding alkynes *6-TMS* and  $(^i\text{Pr}_3\text{Si})\text{C}\equiv\text{C}(\text{SO}_2\text{-}p\text{-C}_6\text{H}_4\text{CH}_3)$  (*6-TIPS*), following the procedure developed by Yamazaki and Wakatsuki for the synthesis of **1**.<sup>10</sup> Table 2 provides a summary of representative spectroscopic data for the cobalt–alkyne complexes *3-TMS* and *3-TIPS* and, for comparison, the symmetrically substituted alkyne complex **1**.<sup>1r</sup> In the IR spectra (KBr) of the polarized alkyne complexes, the  $\nu(\text{C}\equiv\text{C})$  stretching frequency occurs at lower wavenumber by 338–348  $\text{cm}^{-1}$  relative to the free alkyne. In comparison, the symmetrically substituted alkyne complex **1** exhibits a larger wavenumber shift of 403  $\text{cm}^{-1}$  relative to that for  $\text{PhC}\equiv\text{CPh}$  (Raman spectroscopy).<sup>10,6</sup>

Preliminary <sup>13</sup>C NMR chemical shift assignments for the alkyne “sp” carbons in *3-TMS* were made on the basis of the assumption that back-bonding from cobalt to the carbon bearing the electron-withdrawing sulfone substituent would be greater than back-bonding to the carbon bearing the electron-donating TMS substituent. In the <sup>13</sup>C{<sup>1</sup>H} NMR spectra ( $\text{C}_6\text{D}_6$ ) of the sulfone-bearing alkyne complexes *3-TMS* and *3-TIPS*, one of the alkyne “sp” carbon resonances exhibits a small downfield shift ( $\Delta\delta \approx 5\text{--}7$  ppm) and the other a large downfield shift ( $\Delta\delta \approx 15\text{--}17$  ppm), relative to the corresponding chemical shifts in the noncoordinated alkynes. In addition, the downfield resonance exhibits a larger carbon–phosphorus coupling constant than does the upfield resonance.

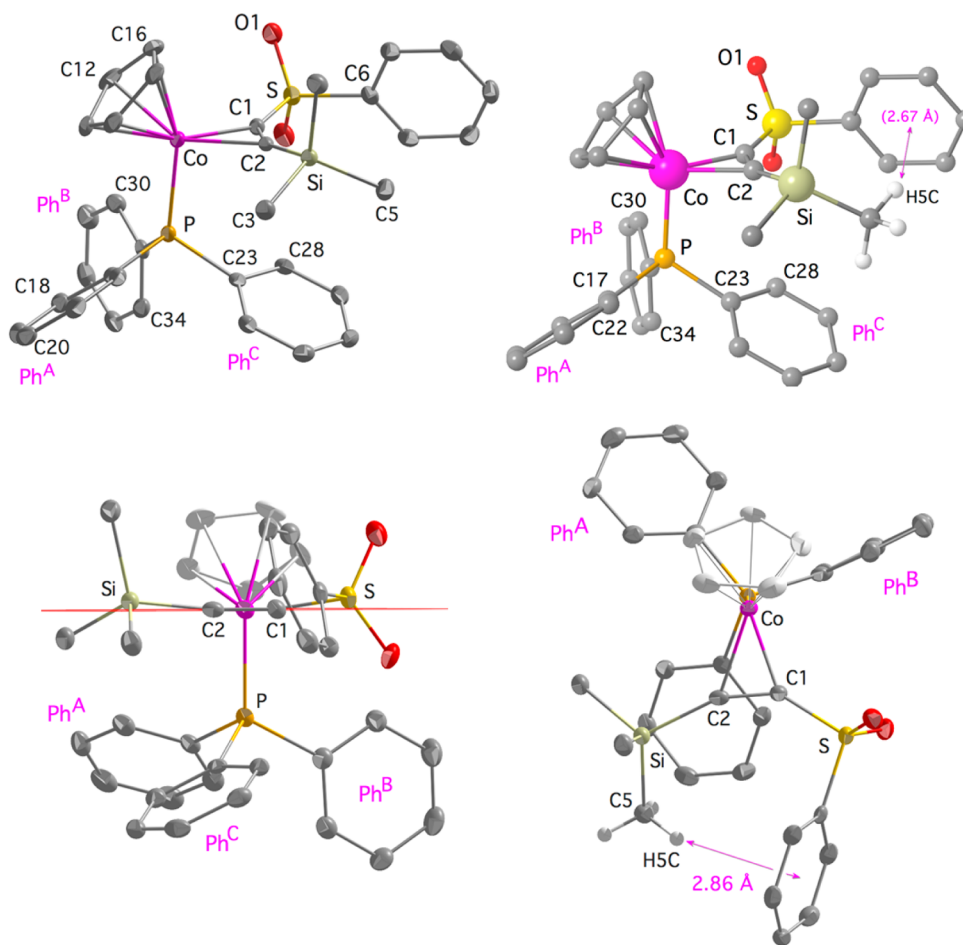


**Figure 2.** ORTEP structure of  $(\eta^5\text{-C}_5\text{H}_5)(\text{PPh}_3)\text{Co}[\eta^2\text{-(TMS)C}\equiv\text{C(SO}_2\text{Ph)}]$  (**3-TMS**; top left), calculated structure of  $(\eta^5\text{-C}_5\text{H}_5)(\text{PPh}_3)\text{Co}[\eta^2\text{-(TMS)C}\equiv\text{C(SO}_2\text{Ph)}]$  (**3-TMS-calc**, ball-and-stick drawing; top right), **3-TMS** viewed down the C1–C2 bond centroid to cobalt axis with the C1–Co–C2 plane highlighted in red (bottom left), and view of **3-TMS** after a  $90^\circ$  rotation of bottom left structure toward the viewer (bottom right). All hydrogen atoms except those on C5 in the right panels have been omitted for clarity.

For comparison,  $(\eta^5\text{-C}_5\text{H}_5)(\text{PPh}_3)\text{Co}(\eta^2\text{-PhC}\equiv\text{CPh})$  (**1**) exhibits a  $^{13}\text{C}$  NMR ( $\text{C}_6\text{D}_6$ ) resonance for the alkyne carbons bound to cobalt at  $\delta$  90.4 ( $J_{\text{PC}} = 8.0$  Hz), which is essentially unchanged from the value for  $\text{PhC}\equiv\text{CPh}$ .<sup>10</sup> Thus, the magnitude of the sp carbon chemical shift change that occurs upon complexation to  $[(\eta^5\text{-Cp})(\text{PPh}_3)\text{Co}]$  depends on the nature of the alkyne substituents, with electron-withdrawing alkyne substituents exhibiting a much larger downfield shift and larger  $^2J_{\text{CP}}$  coupling in comparison to the silyl-substituted carbons.

The chemical shift assignments for **3-TMS** were confirmed by an HMBC NMR experiment (Bruker DRX600 NMR spectrometer with a TXI 5 mm cryoprobe), which demonstrated a correlation between the TMS carbons and the  $\delta$  105.5 alkyne resonance, but not the  $\delta$  118.1 resonance. In routine  $^{13}\text{C}$  NMR spectra, the silicon-29 satellites for the carbon-13 resonances are difficult to detect; however, a  $^{13}\text{C}\{^1\text{H}\}$  NMR spectrum of **3-TMS** obtained on a Varian 500 MHz NMR spectrometer equipped with an X-Sens Cold Probe led to the observation of  $^1J(^{29}\text{Si}^{13}\text{C}) = 40.0$  Hz for the  $\delta$  105.5 resonance. For comparison, the sp carbon bonded to silicon in  $(\text{TMS})\text{C}\equiv\text{C}(\text{C}_6\text{H}_{13})$  exhibits  $^1J(^{29}\text{Si}^{13}\text{C}) = 88.7$  Hz,<sup>7a</sup> and the sp<sup>2</sup> carbon bonded to silicon in ethyl (*E*)-3-(triethylsilyl)-2-propenoate ( $\text{Et}_3\text{SiCH}=\text{CHCO}_2\text{Et}$ ) exhibits  $^1J(^{29}\text{Si}^{13}\text{C}) = 57.9$  Hz.<sup>7b</sup>

**Crystallographic Analysis of the Cobalt–Alkyne Complexes 3-TMS and 3-TIPS.** The only prior solid-state analysis of a  $(\eta^5\text{-Cp})\text{Co}(\text{PPh}_3)(\eta^2\text{-alkyne})$  complex is that reported by Roewer in 2008 for the symmetrically substituted alkyne complex  $(\eta^5\text{-Cp})\text{Co}(\text{PPh}_3)(\eta^2\text{-PhC}\equiv\text{CPh})$  (**1**).<sup>1r</sup> For **3-TMS** the electron-donating trimethylsilyl and electron-withdrawing sulfone substituents are of similar size, as judged in the context of cyclohexane *A* values, which are both 2.5 kcal/mol.<sup>8</sup> The relative sizes of TMS ( $\theta = 118^\circ$ ) and TIPS ( $\theta = 160^\circ$ ) have been addressed in the context of cone angles, with the latter exhibiting a  $42^\circ$  larger cone angle.<sup>9</sup> Although the TIPS group is a slightly better  $\sigma$  donor than TMS, as indicated by a  $4.8\text{ cm}^{-1}$  difference in  $\sigma$  donicity values,<sup>9</sup> the geometric differences in alkyne binding for **3-TMS** relative to **3-TIPS** are expected to be dominated by steric differences associated with the silyl substituents.

The gross solid-state structural features found in **3-TMS** and **3-TIPS** are remarkably similar due to analogous conformations about the P–C, Co–P, and C1–S bonds. The conformation about a triphenylphosphine P–C(ipso) bond is conveniently defined by the angle ( $\omega$ ) between the normals to the Co–P–C<sup>ipso</sup> plane and the phenyl ring least-squares plane.<sup>10</sup> For most triphenylphosphine complexes, the phenyl ring that occupies the least congested site with respect to the other ligands adopts the smallest value for  $\omega$ . Ph<sup>B</sup> is the triphenylphosphine phenyl

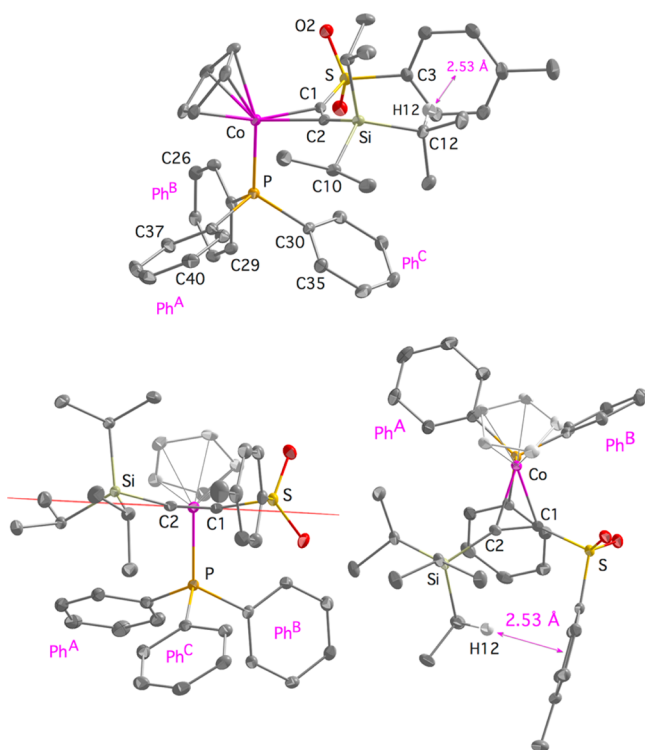


**Figure 3.** ORTEP structure of  $(\eta^5\text{-C}_5\text{H}_5)(\text{PPh}_3)\text{Co}[\eta^2\text{-(TIPS)C}\equiv\text{C(SO}_2\text{Tol)}]$  (**3-TIPS**; top), **3-TIPS** as viewed down the C1–C2 bond centroid to cobalt axis with the C1–Co–C2 plane highlighted in red (bottom left), and view of **3-TIPS** after a  $90^\circ$  rotation of the bottom left structure (bottom right). All hydrogen atoms except those on C12 have been omitted for clarity.

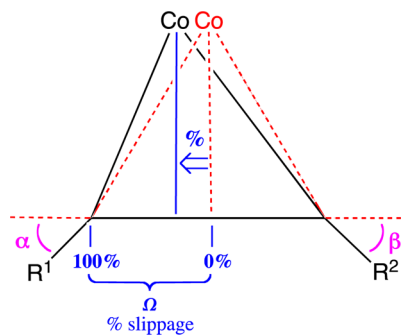


**Figure 4.** Definitions of percent slippage ( $\Omega$ ) and bend-back angles ( $\alpha$  and  $\beta$ ), as applied to Table 4.

**Table 3.** Alkyne Ligand Slippage Parameter ( $\Omega$ ), Substituent Bend-Back Angles ( $\alpha$ ,  $\beta$ ), and Deviations of Alkyne Substituents from the Co–C(1)–C(2) Plane in Cobalt–Alkyne Complexes (See Figure 4)

compd	$\Omega$ slippage, % <sup>a</sup>	$\alpha$ ( $R^1$ ), deg	$\beta$ ( $R^2$ ), deg	$R^1$ deviation, <sup>b</sup> Å	$R^2$ deviation, <sup>b</sup> Å
<b>3-TMS</b>	22	37	23	0.22	0.17
<b>3-TMS-calc</b>	23	37	23	0.21	0.11
<b>5-TMS-calc</b>	9	38	28	0.03	0.04
<b>3-TIPS</b>	28	33	29	0.32	0.32
<b>1</b>	1	31	32	0.16	0.08

<sup>a</sup>For a definition of slippage ( $\Omega$ ) see the text and Figure 4. <sup>b</sup>The  $R^1$  (S or C) and  $R^2$  (Si, C) deviations are from the Co–C1–C2 plane.

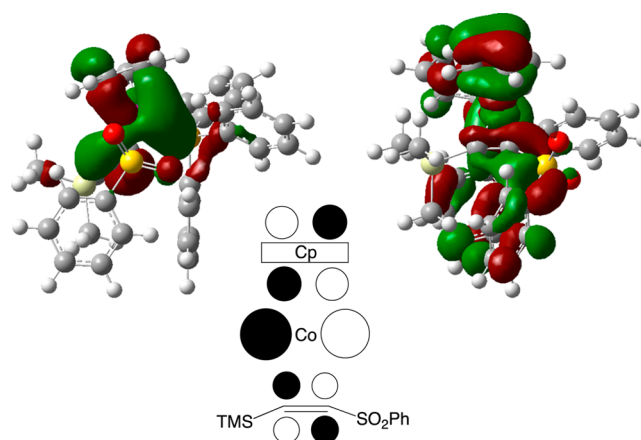


**Figure 5.** (top) Highest occupied molecular orbital (HOMO, left) and lowest unoccupied molecular orbital (LUMO, right) of **3-TMS-calc** (0.02 isosurface). (bottom) Schematic highlighting the common nodal plane in the HOMO of **3-TMS-calc**.

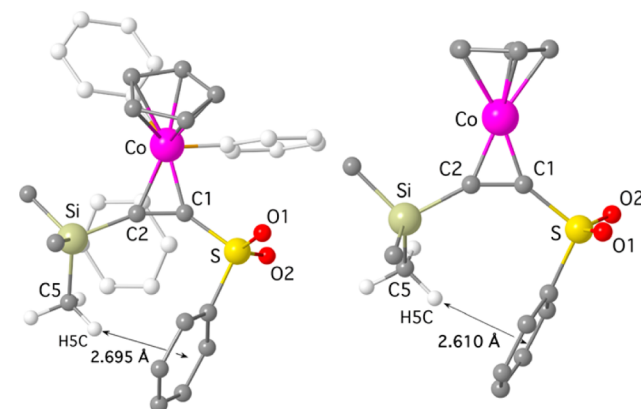


**Figure 6.** B97D/Def2-TZVPP calculated structures of  $(\eta^5\text{-C}_5\text{H}_5)\text{-(PPh}_3\text{)Co}(\eta^2\text{-Me}_3\text{SiC}\equiv\text{CSO}_2\text{Ph})$  (**3-TMS-calc**, left) and  $(\eta^5\text{-C}_5\text{H}_5)\text{-Co}(\eta^2\text{-Me}_3\text{SiC}\equiv\text{CSO}_2\text{Ph})$  (**5-TMS-calc**, right).  $\text{PPh}_3$  carbons are shown in lighter color for clarity; H atoms are omitted except for those on C5.

ring with the smallest  $\omega$  value in both **3-TMS** ( $\omega^A = 57.9^\circ$  ( $\text{Ph}^A$ ,  $57.8^\circ$  calcd);  $\omega^B = 13.3^\circ$  ( $\text{Ph}^B$ ,  $5.4^\circ$  calcd);  $\omega^C = 70.8^\circ$  ( $\text{Ph}^C$ ,  $71.9^\circ$  calcd)) and **3-TIPS** ( $\omega^A = 67.7^\circ$  ( $\text{Ph}^A$ );  $\omega^B = 3.96^\circ$  ( $\text{Ph}^B$ );  $\omega^C = 105.6^\circ$  ( $\text{Ph}^C$ )) (Figures 2 and 3). The similarity in the Co–P conformations observed for **3-TMS** and **3-TIPS** is readily apparent from the C1–Co–P– $\text{Ph}^C$  dihedral angles of  $-84.14$

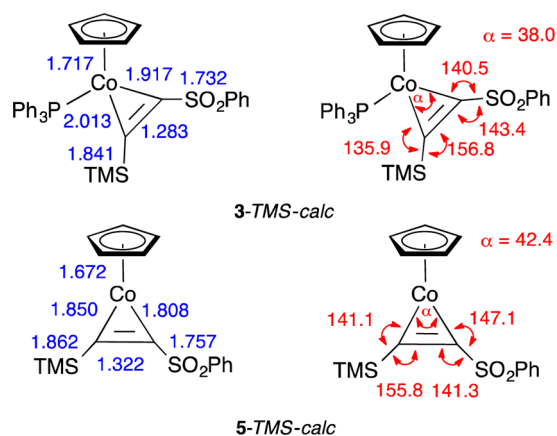


**Figure 7.** Summary of B97D/Def2-TZVPP calculated bond distances (left, Å) and angles (right, deg) for 3-TMS-calc and 5-TMS-calc.

and  $-92.61^\circ$ , respectively. In both complexes the phosphine phenyl ring,  $\text{Ph}^C$ , is positioned below the  $\text{Co}-\text{C}2(\text{SiR}_3)$  bond, with the greater steric bulk of TIPS relative to TMS resulting in a larger  $\omega$  value for  $\text{Ph}^C$  in the 3-TIPS structure ( $\Delta\omega = 34.79^\circ$ ).

The C1-S conformations in 3-TMS and 3-TIPS lead to a folding of the sulfone aryl ring back toward the silyl group, with the closest nonbonded contacts between the sulfone and silyl substituents involving a hydrogen atom of the silyl group and the centroid of the sulfone aryl ring. As seen in Figures 2 and 3, this  $\text{CH}\cdots\pi$  distance is 2.86 Å (2.67 calcd) for 3-TMS and 2.53 Å for 3-TIPS, which are both well within the sum of the van der Waals radii for hydrogen (1.2 Å) and the aromatic ring (1.9 Å).<sup>11</sup> The predicted gas-phase structure, 3-TMS-calc, reproduces this interaction with a  $\text{CH}\cdots\pi$  distance of 2.67 Å (Figure 2, top right). Weak  $\text{CH}/\pi$  interactions (ca. 1 kcal/mol) are often observed in the crystal packing of organometallic complexes.<sup>12</sup> In the case of 3-TMS the similarity of the gas-phase structure to the solid-state structure (Figure 2) indicates

that packing forces are not the primary influence on the observed C-S conformations in the solid-state structures.

The geometric parameters associated with metal-alkyne bonding are defined by the C1-C2, M-C1, and M-C2 distances, by the bend-back angles  $\alpha$  and  $\beta$ , which are a measure of the degree to which the alkyne substituents are bent away from the metal, and by the displacement of the alkyne substituents from the M-C1-C2 plane.

The C $\equiv$ C bond distances in diphenylacetylene (1.192(4) Å) and 6-TMS (1.201(2) Å) are identical within experimental error, as are the corresponding bond distances within **1** (1.278(2) Å), 3-TMS (1.273(3) Å), and 3-TIPS (1.278(3) Å). Pronounced bond length differences are observed for the Co-C1 and Co-C2 bonds in **1** (C1, 1.961(2) Å; C2, 1.955(1) Å) relative to those in 3-TMS (C1, 1.920(2) Å; C2, 2.010(2) Å) and 3-TIPS (C1, 1.919(2) Å; C2, 2.034(2) Å). The observed cobalt-carbon bond distances follow the trend  $\text{Co}-\text{C}(\text{SO}_2\text{Ar}) < \text{Co}-\text{C}_6\text{H}_5 < \text{Co}-\text{C}(\text{SiR}_3)$ , which follows the expected inverse correlation with the anticipated degree of cobalt-carbon back-bonding. The steric effect of the TIPS group relative to the TMS group results in a significantly longer Co-C1(TIPS) bond distance relative to the Co-C1(TMS) bond distance.

Both steric and electronic factors may impact the magnitude of the bend-back angle; however, in cases with two large alkyne substituents, such as in 3-TMS and 3-TIPS,  $\alpha$  and  $\beta$  may also be influenced by steric congestion between the two alkyne substituents. For both complexes of **3**,  $\alpha$  is substantially larger than  $\beta$ , which may be attributed primarily to greater back-donation to C1(SO<sub>2</sub>Ar) than to C2(SiR<sub>3</sub>). The larger  $\alpha$  value for 3-TMS ( $37^\circ$ ) relative to 3-TIPS ( $31^\circ$ ) is attributed to greater steric congestion between the sulfone and silyl substituents in the latter complex. For 3-TIPS,  $\beta$  is  $6^\circ$  larger than in the case of 3-TMS, as is to be expected on the basis of the relative sizes of the TMS and TIPS groups.

A convenient structural parameter that encompasses many of the individual bond distance and angle metrics associated with alkyne coordination is the *alkyne-slippage* parameter ( $\Omega$ ),

**Table 4.** Selected Distances (Å) and Angles (deg) for the  $(\eta^5\text{-C}_5\text{H}_5)(\text{PPh}_3)\text{Co}(\eta^2\text{-R}^1\text{C}\equiv\text{CR}^2)$  Complexes As Determined by Crystallography and/or Computation

	<b>1</b>	3-TIPS	3-TMS [3-TMS-calc] <sup>a</sup>	5-TMS-calc
C1-C2	1.2779(19)	1.278(3)	1.273(3) [1.283] <sup>a</sup>	[1.322] <sup>a</sup>
Co-C1	1.9614(13)	1.919(2)	1.920(2) [1.918]	[1.808]
Co-C2	1.9548(13)	2.034(2)	2.010(2) [2.014]	[1.850]
C1-R <sup>1</sup>	1.955(1)	1.731(2)	1.718(2) [1.731]	[1.757]
C2-R <sup>2</sup>	1.961(1)	1.867(2)	1.853(2) [1.842]	[1.862]
Co-P	2.1573(4)	2.170(1)	2.178(1) [2.151]	
S-O(1)		1.445(1)	1.445(2) [1.456]	1.450
S-O(2)		1.447(2)	1.446(2) [1.456]	1.451
C1-C2-R <sup>2</sup>	149.29(13)	150.8(1)	157.4(2) [156.813]	[151.72]
C2-C1-R <sup>1</sup>	147.65(13)	147.4(1)	143.0(2) [143.365]	[142.32]
Co-C1-C2	70.68(8)	76.1(1)	75.0(1) [75.069]	[70.52]
Co-C2-C1	71.23(8)	66.3(1)	67.3(1) [66.941]	[67.13]
Co-C1-R <sup>1</sup>	140.69(10)	134.0(1)	140.8(1) [140.480]	[147.13]
Co-C2-R <sup>2</sup>	139.22(10)	140.2(1)	134.5(1) [135.895]	[141.12]

<sup>a</sup>Values in brackets are for the calculated structures.

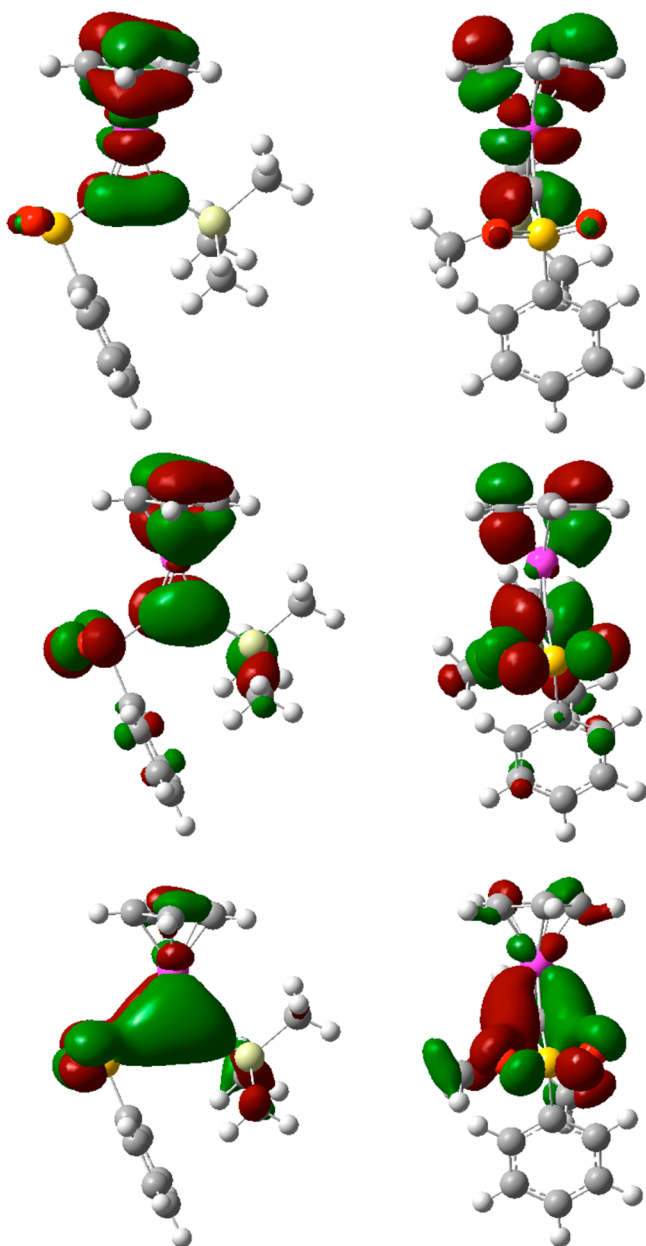


**Figure 8.** Molecular orbitals (0.03 isosurface, two views) indicative of a three-center–four-electron bonding interaction in *5-TMS-calc*: LUMO (top), HOMO-5 (middle), and HOMO-15 (bottom).

previously developed by Gladysz (Figure 4 and Table 3).<sup>4</sup> For metal–alkyne complexes the slippage value would be 0% when the perpendicular from cobalt to the C1–C2 bond intercepts the C≡C midpoint, as in an equilateral triangle (red dashed lines in Figure 4). As expected,  $\Omega \approx 0$  for the symmetrically substituted alkyne complex **1**. When slippage occurs, the Co–C1–C2 three-membered ring takes the form of a scalene triangle (black triangle in Figure 4). The slippage value would be 100% if the perpendicular shown in blue intersects at C1 or C2. Alkyne slippage is greater in *3-TIPS* (28%) than *3-TMS* (22%), primarily due to the greater size of TIPS relative to TMS.

**Calculated Structures for  $(\eta^5\text{-Cp})(\text{PPh}_3)\text{Co}\{\eta^2\text{-(Me}_3\text{Si)C}\equiv\text{C(SO}_2\text{Ph)}\}$  (*3-TMS-calc*) and  $(\eta^5\text{-Cp})\text{Co}\{\eta^2\text{-(Me}_3\text{Si)C}\equiv\text{C(SO}_2\text{Ph)}\}$  (*5-TMS-calc*).** In order to determine the structural and electronic changes to alkyne coordination that occur upon

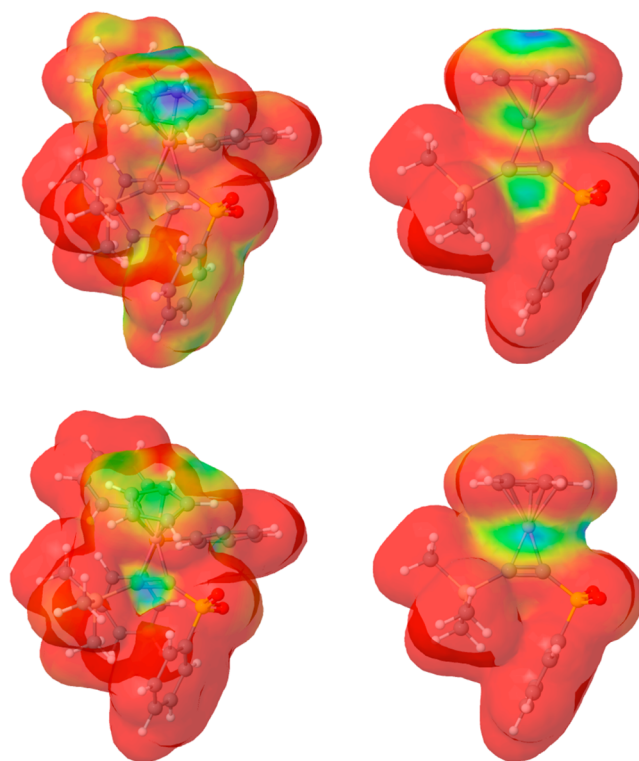


**Figure 9.** (bottom) Electrophilic HOMO frontier density plots for *3-TMS-calc* and *5-TMS-calc*. (top) Nucleophilic LUMO frontier density plots for *3-TMS-calc* and *5-TMS-calc*.

dissociation of  $\text{PPh}_3$  from *3-TMS-calc* and  $(\eta^5\text{-Cp})\text{Co}\{\eta^2\text{-(Me}_3\text{Si)C}\equiv\text{C(SO}_2\text{Ph)}\}$  (*5-TMS-calc*; Figures 5–7) were compared. Figure 5 shows the frontier orbitals for *3-TMS-calc*, from which one can observe a nodal pattern in the HOMO (left upper panel), as depicted at the bottom of the figure, and the LUMO showing very little orbital density on the alkyne ligand (top right), with a larger component on C2 than on C1.

The calculated dipole moments for **6-TMS** (5.72 D), **3-TMS** (4.92 D), and *5-TMS-calc* (4.94 D) are similar, and in the case of the two alkyne complexes they are nearly identical. However, significant differences in alkyne coordination are observed for *3-TMS-calc* and *5-TMS-calc*. The calculated structure for *5-TMS-calc* exhibits a nearly linear Cp–Co–alkyne geometry with a  $177.4^\circ$  Cp(centroid)–Co–alkyne (C1–C2 midpoint) angle, with the degree of alkyne slippage reduced significantly from  $\Omega = 22\%$  in *3-TMS-calc* to  $\Omega = 9\%$  in *5-TMS-calc* (Table 3 and Figure 6). A second conformer very close in energy to the one shown for *5-TMS-calc* has the phenyl ring rotated away from the TMS group, indicative of a very minor preference for the conformer shown in Figure 6.

Four-electron-donor alkyne ligands typically exhibit longer C1–C2 and shorter C–M bond distances relative to those observed for related complexes involving two-electron-donor alkyne ligands.<sup>13</sup> A comparison of these bond distances for *3-TMS-calc* and *5-TMS-calc* reveals a significantly longer C1–C2 bond distance ( $\Delta = 0.039 \text{ \AA}$ ) and significantly shorter Co–C1(TMS) ( $\Delta = -0.109$ ) and Co–C2(SO<sub>2</sub>Ph) ( $\Delta = -0.151 \text{ \AA}$ ) distances in the phosphine-dissociated complex (Figures 6 and 7 and Table 4), all of which are consistent with a four-electron-donor alkyne ligand. In addition, the C1/C2 chemical shifts in the <sup>13</sup>C NMR spectra of four-electron-donor alkyne complexes typically resonate significantly downfield of those for two-electron-donor alkyne ligands.<sup>13a</sup> In the case of *5-TMS-calc*, the

calculated carbon-13 chemical shifts for C1(SO<sub>2</sub>Ph) (175.9 ppm) and C2(TMS) (190.7 ppm) are 63–76 ppm downfield of the corresponding chemical shifts found for 3-*TMS-calc* (C1, 113.0 ppm; C2, 115.0 ppm), once again consistent with a four-electron-donor alkyne ligand.

The formulation of the alkyne ligand in 5-*TMS-calc* as a four-electron-donor alkyne ligand is further supported by an analysis of the calculated molecular orbitals (Figure 8). Electron donation from the  $\pi_{\perp}$  orbital of the alkyne breaks the degeneracy of the cobalt  $d_{xz}$  and  $d_{yz}$  orbitals, thereby leading to a singlet configuration. The cobalt d orbital (e.g., the  $d_{yz}$  orbital) that accepts the  $\pi_{\perp}$  electrons is also involved as an acceptor of  $\pi$  electrons from the Cp ligand. The resultant three-orbital–four-electron interaction is described by the LUMO, HOMO-5, and HOMO-15 molecular orbitals. The LUMO is the totally antibonding component of the three-center–four-electron interaction. This orbital shows that a nucleophile would be expected to attack at the alkyne, at the cyclopentadienyl ligand, or at cobalt. For alkyne nucleophiles, attack at cobalt would give bis(alkyne) complexes that are proposed as key intermediates in alkyne cyclotrimerizations. HOMO-5 is alkyne- $\pi$  and Cp- $\pi$  in character with a node at cobalt, and HOMO-15 represents the fully bonding descriptor of the three-center–four-electron interaction in which there is an alkyne out-of-plane  $\pi$  interaction with the cobalt  $d_{yz}$  orbital.

The electrophilic HOMO frontier density plots for 3-*TMS-calc* and 5-*TMS-calc* (Figure 9, bottom) indicate a greater probability of attack by an electrophile (in the absence of steric effects) at C2 in 3-*TMS-calc*, whereas in the phosphine-dissociated analogue 5-*TMS-calc* there is a greater probability of attack by an electrophile at cobalt. The nucleophilic LUMO frontier density plots for 3-*TMS-calc* and 5-*TMS-calc* (Figure 9, top) indicate that the probability of attack by a nucleophile at the alkyne carbons in 5-*TMS-calc* is greater than in 3-*TMS-calc*; however, alkyne nucleophiles would be expected to attack 5-*TMS-calc* at cobalt (as discussed above for the LUMO shown in Figure 8).

## SUMMARY

The first X-ray crystallographic and computational studies on  $(\eta^5\text{-Cp})(\text{PPh}_3)\text{Co}(\eta^2\text{-alkyne})$  complexes of unsymmetrically substituted alkynes are reported. The calculated structure of the phosphine-dissociated complex  $(\eta^5\text{-C}_5\text{H}_5)\text{Co}(\eta^2\text{-Me}_3\text{SiC}\equiv\text{CSO}_2\text{Ph})$  (5-*TMS-calc*) reveals the presence of a four-electron-donor alkyne ligand. A comparison of the calculated structures for 3-*TMS-calc* and 5-*TMS-calc* demonstrates a significant decrease in the alkyne slippage parameter, which may be attributed to the effect of electron donation from the  $\pi_{\perp}$  orbital to cobalt. Studies are in progress to determine if this phenomenon is a general one for other four-electron-donor alkyne ligands bearing polarizing alkyne substituents.

## EXPERIMENTAL SECTION

**Computational Methods.** The conformational analyses of the molecular systems described in this study, including structural and orbital arrangements as well as property calculations, were carried out using the GAMESS<sup>14</sup> and GAUSSIAN09<sup>15</sup> software packages. Structural computations of all compounds were performed using the B97-D dispersion enabled density functional method, with an ultrafine grid, in accord with the ansatz proposed by Grimme.<sup>16,17</sup> The B97-D exchange-correlation functional is a special reparameterization of the original B97 hybrid functional of Becke,<sup>18</sup> which is more neutral to spurious dispersion contamination in the exchange part than the original functional. The Def2-TZVPP basis set<sup>19</sup> was used for all

calculations. Full geometry optimizations were performed and uniquely characterized via second derivatives (Hessian) analysis to determine the number of imaginary frequencies (0 = minima; 1 = transition state), and effects of zero-point energy. From the fully optimized structures, single-point NMR computations were performed with the class II NMR methodology, CSGT,<sup>20</sup> and calibrated against TMS. Visualization and analysis of structural and property results, including electrophilic (HOMO) and nucleophilic (LUMO) frontier density plots, were obtained using Avogadro<sup>21</sup> and WEBMO.<sup>22</sup>

## ASSOCIATED CONTENT

### Supporting Information

CIF files giving X-ray crystallographic data. This material is available free of charge via the Internet at <http://pubs.acs.org>.

## AUTHOR INFORMATION

### Corresponding Authors

\*E-mail for K.K.B.: [kimb@oci.uzh.ch](mailto:kimb@oci.uzh.ch).

\*E-mail for J.M.O.: [jmoconnor@ucsd.edu](mailto:jmoconnor@ucsd.edu).

### Notes

The authors declare no competing financial interest.

## ACKNOWLEDGMENTS

We thank the NSF (grant CHE-1214024) and the Swiss National Science Foundation (K.K.B.) for support of this work. C.L.V. was supported by a National Science Foundation GK12 Grant (DGE-0742551). We thank Profs. Joshua Figueroa and Jay Siegel for helpful discussions.

## REFERENCES

- (1) (a) Yamazaki, H.; Hagihara, N. *J. Organomet. Chem.* **1967**, *7*, P22. (b) Yamazaki, H.; Hagihara, N. *J. Organomet. Chem.* **1970**, *21*, 431. (c) Yamazaki, H.; Hagihara, N. *Bull. Chem. Soc. Jpn.* **1971**, *44*, 2260. (d) Wakatsuki, Y.; Yamazaki, H.; Iwasaki, H. *J. Am. Chem. Soc.* **1973**, *95*, 5781. (e) Yasufuku, K.; Yamazaki, H. *J. Organomet. Chem.* **1976**, *i*, 405. (f) Yamazaki, H.; Wakatsuki, Y. *J. Organomet. Chem.* **1977**, *139*, 157. (g) Yasufuku, K.; Yamazaki, H. *J. Organomet. Chem.* **1977**, *127*, 197. (h) Wakatsuki, Y.; Yamazaki, H. *J. Organomet. Chem.* **1977**, *i*, 169. (i) Yamazaki, H.; Wakatsuki, Y. *J. Organomet. Chem.* **1978**, *149*, 377. (j) Hong, P.; Aoki, K.; Yamazaki, H. *J. Organomet. Chem.* **1978**, *150*, 279. (k) Wakatsuki, Y.; Yamazaki, H. *J. Organomet. Chem.* **1978**, *149*, 385. (l) McDonnell Bushnell, L. P.; Evitt, E. R.; Bergman, R. G. *J. Organomet. Chem.* **1978**, *157*, 445. (m) Wakatsuki, Y.; Aoki, K.; Yamazaki, H. *J. Am. Chem. Soc.* **1979**, *101*, 1123. (n) Wakatsuki, Y.; Nomura, O.; Kitaura, K.; Morokuma, K.; Yamazaki, H. *J. Am. Chem. Soc.* **1983**, *105*, 1907. (o) Yamazaki, H.; Wakatsuki, Y. *J. Organomet. Chem.* **1984**, *272*, 251. (p) Wakatsuki, Y.; Miya, S.; Ikuta, S.; Yamazaki, H. *J. Chem. Soc., Chem. Commun.* **1985**, *35*. (q) Wakatsuki, Y.; Miya, S.; Yamazaki, H.; Ikuta, S. *J. Chem. Soc., Dalton Trans.* **1986**, *1201*. (r) Wakatsuki, Y.; Miya, S.; Yamazaki, H. *J. Chem. Soc., Dalton Trans.* **1986**, *1207*. (s) Wakatsuki, Y.; Aoki, K.; Yamazaki, H. *J. Chem. Soc., Dalton Trans.* **1986**, *1193*. (t) Stolzenberg, A. M.; Scozzafava, M.; Foxman, B. M. *Organometallics* **1987**, *6*, 769. (u) Scozzafava, M.; Stolzenberg, A. M. *Organometallics* **1988**, *7*, 1073. (v) Wakatsuki, Y.; Yamazaki, H. *Inorg. Syn.* **1989**, *26*, 189. (w) O'Connor, J. M.; Chen, M.-C.; Frohn, M.; Rheingold, A. L.; Guzei, I. A. *Organometallics* **1997**, *16*, 5589. (x) O'Connor, J. M.; Chen, M.-C.; Rheingold, A. L. *Tetrahedron Lett.* **1997**, *38*, 5241. (y) Baldrige, K. K.; O'Connor, J. M.; Chen, M.-C.; Siegel, J. S. *J. Phys. Chem. A* **1999**, *103*, 10126. (z) Hoffman, F.; Wagler, J.; Roewer, G. Z. *Anorg. Allg. Chem.* **2008**, *634*, 1133. (aa) O'Connor, J. M.; Bunker, K. D.; Rheingold, A. L.; Zakharov, L. J. *J. Am. Chem. Soc.* **2005**, *127*, 4180. (ab) O'Connor, J. M.; Chen, M.-C.; Holland, R. L.; Rheingold, A. L. *Organometallics* **2011**, *30*, 369. (2) (a) O'Connor, J. M.; Ji, H.; Iranpour, M.; Rheingold, A. L. *J. Am. Chem. Soc.* **1993**, *115*, 1586. (b) O'Connor, J. M.; Baldrige, K. K.;



Vélez, C. L.; Rheingold, A. L.; Moore, C. E. *J. Am. Chem. Soc.* **2013**, *135*, 8826.

(3) Gandon, V.; Agenet, N.; Vollhardt, K. P. C.; Malacria, M.; Aubert, C. *J. Am. Chem. Soc.* **2006**, *128*, 8509.

(4) (a) Boone, B. J.; Klein, D. P.; Seyler, J. W.; Mendez, N. Q.; Arif, A. M.; Gladysz, J. A. *J. Am. Chem. Soc.* **1996**, *118*, 2411. (b) Kowalczyk, J. J.; Arif, A. M.; Gladysz, J. A. *Organometallics* **1991**, *10*, 1079.

(5) Hansch, C.; Leo, A.; Taft, R. W. *Chem. Rev.* **1991**, *91*, 165.

(6) Van Gaal, H. L. M.; Graef, M. W. M.; van der Ent, A. J. *Organomet. Chem.* **1977**, *131*, 453.

(7) (a) Kamienska-Trela, K.; Biedrzycka, Z.; Machinek, R.; Knieriem, B.; Luetke, W. *Org. Magn. Reson.* **1984**, *22*, 317. (b) Liepins, E.; Birgele, I.; Lukevics, E.; Sheludyakov, V. D.; Lahtin, V. G. *J. Organomet. Chem.* **1990**, *385*, 185.

(8) (a) Kitching, W.; Olszowy, H. A.; Drew, G. M. *J. Org. Chem.* **1982**, *47*, 5153. (b) Eliel, E. L.; Allinger, N. L.; Angyal, S. J.; Morrison, G. A. *Conformational Analysis*; Interscience: New York, 1965.

(9) Rücker, C. *Chem. Rev.* **1995**, *95*, 1009.

(10) For a slightly different definition of  $\omega$  and a detailed analysis of PPh<sub>3</sub> ligand conformations in organometallic complexes see: (a) Costello, J. F.; Davies, S. G. *J. Chem. Soc., Perkin Trans. 2* **1998**, 1683. (b) Costello, J. F.; Davies, S. G.; McNally, D. *J. Chem. Soc., Perkin Trans. 2* **1999**, 465.

(11) Pauling, L. *The Nature of the Chemical Bond*; Cornell University Press: Ithaca, NY, 1960; p 260.

(12) (a) Suezawa, H.; Yoshida, T.; Umezawa, Y.; Tsuboyama, S.; Nishio, M. *Eur. J. Inorg. Chem.* **2002**, 3148. (b) Dunitz, J. D.; Gavezzotti, A. *Cryst. Growth Des.* **2005**, *5*, 2180. (c) Tsuzuki, S.; Fujii, A. *Phys. Chem. Chem. Phys.* **2008**, *10*, 2584.

(13) (a) Templeton, J. L. *Adv. Organomet. Chem.* **1989**, *29*, 1. (b) Marinelli, G.; Streib, W. E.; Huffman, J. C.; Caulton, K. G.; Gagné, Takats, J.; Dartiguenave, M.; Chardon, C.; Jackson, S. A.; Eisenstein, O. *Polyhedron* **1990**, *9*, 1867.

(14) Schmidt, M. W.; Baldrige, K. K.; Boatz, J. A.; Elbert, S. T.; Gordon, M. S.; Jensen, J. H.; Koseki, S.; Matsunaga, N.; Nguyen, K. A.; Su, S.; Windus, T. L.; Elbert, S. T. *J. Comput. Chem.* **1993**, *14*, 1347.

(15) *Gaussian 09*; Gaussian, Inc., Wallingford, CT, 2009.

(16) Grimme, S. *J. Comput. Chem.* **2006**, *27*, 1787–1799.

(17) Grimme, S. *J. Chem. Phys.* **2006**, *124*, 034108–034115.

(18) Becke, A. D. *J. Chem. Phys.* **1997**, *107*, 8554–8560.

(19) Weigend, F.; Ahlrichs, R. *Phys. Chem. Chem. Phys.* **2005**, *7*, 3297–3305.

(20) Keith, T. A.; Bader, R. F. W. *Chem. Phys. Lett.* **1993**, *210*, 223.

(21) Hanwell, M.; Curtis, D.; Lonie, D.; Vandermeersch, T.; Zurek, E.; Hutchison, G. *J. Cheminform.* **2012**, *4*, 17.

(22) WEBMO: Cundari, T.; Schmidt, J. R. [www.webmo.net](http://www.webmo.net).